Corrosion mechanisms in aqueous solutions containing dissolved H2S. Part 1: Characterisation of H2S reduction on a 316L rotating disc electrode.

Jean Kittel, François Ropital, François Grosjean, Eliane Sutter, Bernard Tribollet

Corrosion mechanisms in aqueous solutions containing dissolved H_2S. Part 1: Characterisation of H_2S reduction on a 316L rotating disc electrode.

J. Kittel*, F. Ropital, F. Grosjean
IFP Energies nouvelles, Rond-point de l'échangeur de Solaize BP3, 69360 Solaize, France

E.M.M. Sutter, B. Tribollet
Laboratoire Interfaces et Systèmes Electrochimiques, UPR 15 du CNRS, 75252 Paris Cedex 05

Abstract

This paper compares the cathodic reactions occurring on steel in aqueous solution containing dissolved H_2S or CO_2. In aqueous solutions containing these weak acids, the rate of the cathodic reaction is enhanced in comparison with strong acid solutions at the same pH. In the case of dissolved CO_2, this phenomenon is fully explained by a buffer effect, contributing to the transport of proton at the steel surface. In the case of H_2S containing solutions, this chemical mechanism is no more sufficient to explain the cathodic polarization curves. An additional electrochemical reaction is clearly observed, with strong links with H_2S concentration.

Keywords

B. electrochemical calculation ; B. modelling studies ; B. Polarization ; C. acid corrosion

Introduction

Corrosion in oil and gas environments very often involves water with dissolved CO_2 and H_2S. Once dissolved in water, both CO_2 and H_2S behave like weak acids. As such, they are able to provide oxidizing power and promote iron corrosion, establishing an equilibrium between oxidation and reduction reactions:

$$Fe \rightarrow Fe^{2+} + 2e^- \quad (1)$$

The most common reduction reaction in de-aerated acid media is proton reduction:

$$H^+ + e^- \rightarrow \frac{1}{2}H_2 \quad (2)$$

* Corresponding author: jean.kittel@ifpen.fr – Phone +33 (0)4 37 70 27 83

However, additional reactions might take place. This subject has been widely discussed for CO_2, starting several decades ago [1-12]. One particular aspect with CO_2 corrosion is the fact that it is usually enhanced in comparison with strong acid solutions at the same pH. This trend is extremely well established, in particular in the oil and gas industry. However, this mechanism remains poorly understood. Two major theories coexist to explain this additional corrosivity in carbonic acid solutions. Until very recently, the most common assumption consisted in considering that carbonic acid could be reduced:

$$H_2CO_3 + e^- \rightarrow HCO_3^- + \frac{1}{2}H_2 \quad (3)$$

This cathodic reaction would thus be added to proton reduction (2), thereby increasing the global cathodic current.

However, recent results obtained by the authors showed that the additional cathodic current could entirely be explained by mass transport and chemical kinetics [10]. The model that was described contains one unique charge transfer reaction (2), while the mass transfer limitation contains diffusion of H^+ and diffusion of the weak acid (dissolved CO_2) from the bulk of the solution. Quantitatively, for a pH level and CO_2 partial pressure (P_{CO2}) typical of oil and gas fields, transport of acidity at the steel surface is attributed in majority to CO_2 rather than to H^+: e.g. at ambient temperature under 1 bar CO_2 at pH 4, CO_2 concentration in pure water is 3.3×10^{-2} mol/L, while H^+ concentration is only 10^{-4} mol/L. Thus, CO_2 provides an additional source of protons at the steel surface by transport of CO_2 from the bulk followed by chemical dissociation reactions:

$$CO_2 + H_2O \rightleftharpoons H^+ + HCO_3^- \quad (4)$$

$$HCO_3^- \rightleftharpoons H^+ + CO_3^{2-} \quad (5)$$

This dissociation reaction has a slow kinetics: it represents the rate determining step for the CO_2 contribution, rather than CO_2 transport itself.
The same kind of chemical contribution has been observed recently for acetic acid [13].

To our knowledge, only few papers in the literature describe the cathodic reactions in water containing dissolved H_2S.
In the 60's, Bolmer proposed a direct reduction reaction as [14]:

$$H_2S + e^- \rightarrow HS^- + \frac{1}{2}H_2 \quad (6)$$

Polarization tests were conducted in stagnant condition in near neutral solutions containing different amount of H_2S and HS^-. Bolmer reported Tafel slopes between 115 mV and 55 mV depending on HS^- concentration. Mass transfer limitation was also observed, but it could not be interpreted quantitatively.

In the eighties, Morris et al. used a carbon steel rotating disc electrode to study corrosion in aqueous H_2S systems of acid pH [15]. They concluded that H_2S did not modify the cathodic process in the activation region, but they noticed also that H^+ diffusion control disappeared gradually with H_2S.
Measurements in controlled turbulent flow conditions were reported by Galvan-Martinez et al. [16], with a rotating cylinder made of carbon steel. They examined the hypothesis of a direct H_2S reduction according to Equation (6), but they noticed that the corrosion potential was situated in a region where the cathodic current was under H^+ mass transfer limitation.
Another mechanism of H_2S contribution was proposed by Shoesmith et al. These authors stated that corrosion reaction of iron with H_2S occurred mainly by a solid state reaction, via the global reaction scheme [17]:

$$Fe + H_2S \rightarrow FeS + H_2 \quad (7)$$

This reaction is still adopted in most of experimental work on iron corrosion in the presence of H_2S, considering that formation of a protective mackinawite scale is the main parameter for corrosion control, rather than electrochemical kinetics [8,18].
Other studies dealt with cathodic reactions in H_2S containing solutions, but they were focused on the impact of H_2S on hydrogen recombination or charging in the steel, causing embrittlement [6,19-23].

Lastly, it was never mentioned in the literature that a buffer behaviour similar to CO_2 could also be proposed. H_2S would then only contribute through its dissociation reactions as an additional source of protons at the corroding surface:

$$H_2S \rightleftharpoons H^+ + HS^- \quad (8)$$

$$HS^- \rightleftharpoons H^+ + S^{2-} \quad (9)$$

The main objective of this paper is to examine the nature of the impact of H_2S on the cathodic reactions in acidic solution. It will be compared with the reference case of CO_2.

Experimental

Experiments were performed using a 316L rotating disc electrode (RDE) as working electrode. Before each experiment, the electrode surface was grinded with 1200 grit paper, degreased with acetone and rinsed with deionised water. The chemical composition of the steel is given in Table 1.

Table 1: Chemical composition (wt%) of the 316L working electrode

C	Si	Mn	Ni	Cr	Mo	N	S	P
0.021	0.37	1.34	10.05	16.53	2.02	0.036	0.03	0.031

The supporting electrolyte was a 0.01M K_2SO_4 solution. Before each experiment, this solution was de-aerated by purging N_2 for at least 2 hours. The solution was then saturated with H_2S at different concentrations, by purging with different ratios of N_2 and H_2S, from 0.1% H_2S to 5 % H_2S, corresponding respectively to a partial pressure of H_2S (P_{H2S}) of 1 mbar and 50 mbar, or to 10^{-4} mol/L to $5x10^{-3}$ mol/L of dissolved H_2S. Continuous bubbling of the gas was maintained during all the experiment to keep a constant concentration of dissolved H_2S.
The pH of the test solution was then adjusted to target value between 4 and 6 by KOH or H_2SO_4 addition. Test solution transfer from the preparation tank to the de-aerated electrochemical cell was realized without contacting the solution with air, to avoid any reaction of dissolved H_2S with oxygen, and prevent oxygen reduction contribution during electrochemical measurements.
All experiments were carried out at room temperature (23 +/- 2℃) using a conventional three-electrode cell. A Ag/AgCl reference filled with saturated KCl solution and a large platinum grid were used as reference and counter electrodes, respectively. The equipment for electrochemical measurement was a Biologic SP200 potentiostat monitored with EC-Lab software. Potential sweeps were performed at a rate of 1 mV/s.
All experiments were conducted in a laboratory equipped with H_2S detection and appropriate protection equipment. All gaseous effluents containing H_2S were collected and neutralized by a sodium hydroxide solution.

Results and discussion

Typical cathodic experimental stationary polarization curves measured on a 316L steel rotating disk electrode in solutions at pH 4 and with or without 9 mbar H_2S are presented in Figure 1.
Without H_2S, the polarization curve shows a well defined current plateau due to proton reduction, followed by water reduction in the lower cathodic potential range. The current plateau can be ascribed to the mass transport of proton, since it follows strictly the Levich relation [24]:

$$J_{\lim,H^+} = 0.62FC_{H^+_{bulk}} D_{H^+}^{2/3} \upsilon^{-1/6} \omega^{1/2} \qquad (10)$$

where $J_{\lim,H^+}$ is the diffusion limited current for H^+ reduction, F is the Faraday constant (96500 C/mol), $C_{H^+_{bulk}}$ is the bulk concentration of protons, D_{H^+} is the diffusion coefficient of H^+, υ is the kinematic viscosity of the liquid, and ω is the angular rotation speed of the electrode.

The addition of 9 mbar H_2S modifies considerably the polarization curves. The current plateau due to H^+ reduction is no more well defined and a second wave appears at more cathodic potentials, which should be attributed to the electroactivity of H_2S.

Similar observations were made recently at more acidic pH and with carbon steel rotating cylinder devices, showing also an electrochemical activity of H_2S [25].

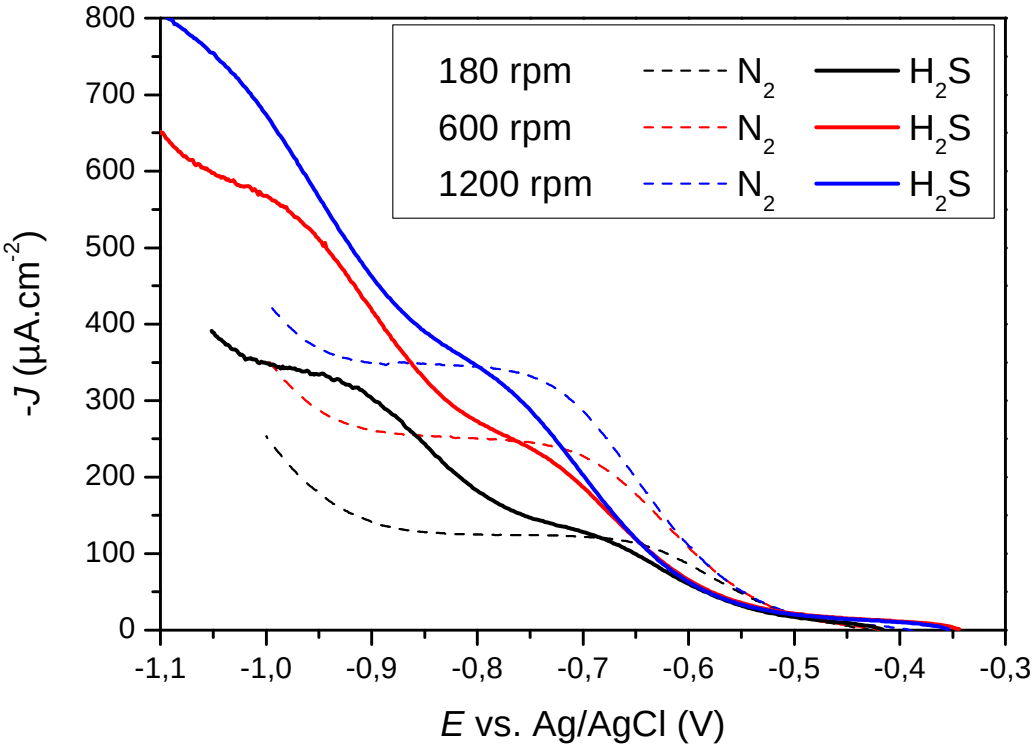

Figure 1 : Stationary cathodic polarization curves measured with a RDE at pH 4 in N_2 purged solution or in H_2S saturated (9 mbar) solution

In order to characterize in more details the electrochemical reactions associated with H_2S, additional experiments were performed in less acidic solutions, or with different P_{H2S}. The corresponding polarization curves are presented in Figure 2 and Figure 3, respectively.

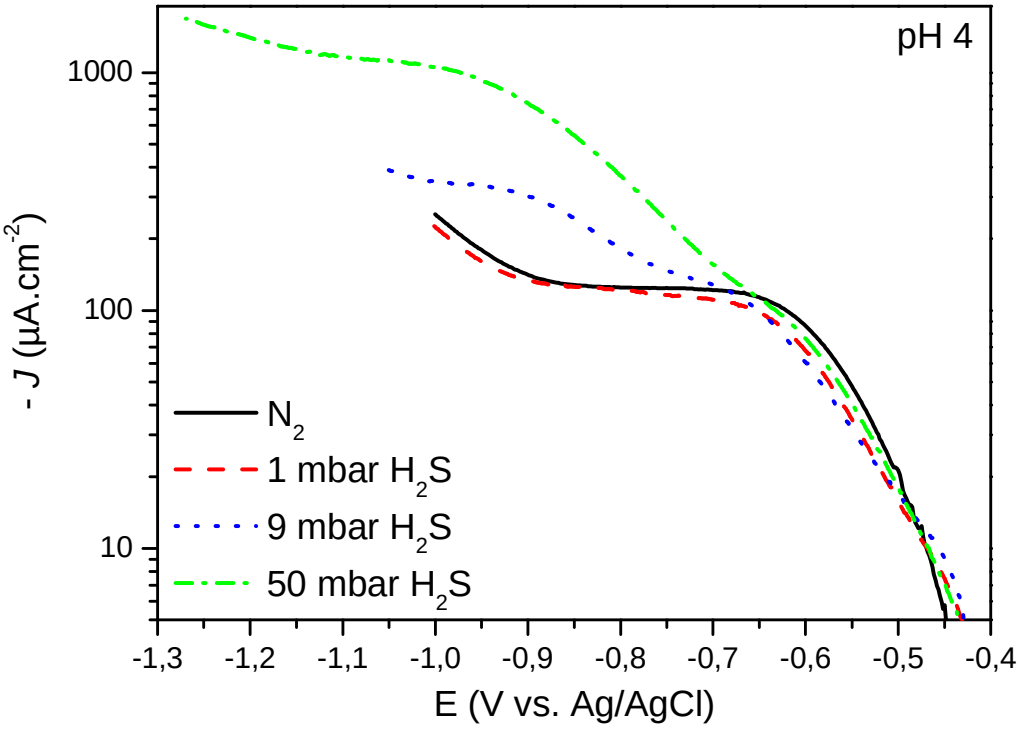

Figure 2: Stationary cathodic polarization curves measured with a RDE at 180 rpm in de-aerated solution containing different amount of H_2S at pH 4

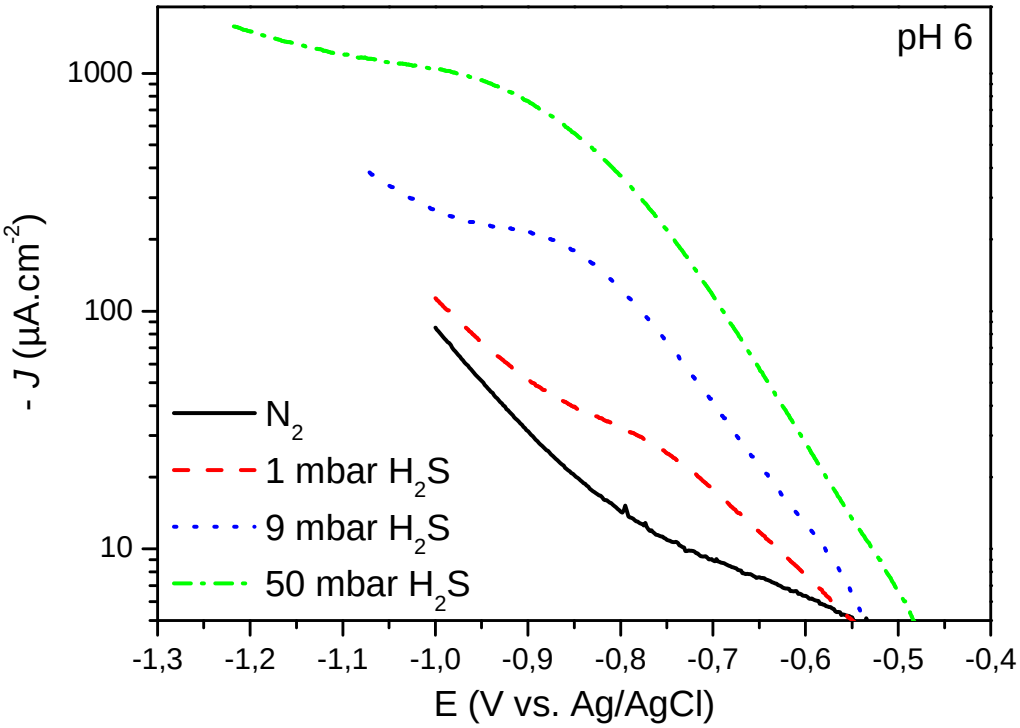

Figure 3: Stationary cathodic polarization curves measured with a RDE at 180 rpm in de-aerated solution containing different amount of H_2S at pH 6

In the presence of dissolved H_2S, an additional cathodic contribution appears on the polarization curves.
At pH 4, and for P_{H2S} between 1 mbar and 50 mbar, the additional electrochemical reaction associated with H_2S reduction takes place in the potential domain of mass transport limitation of the proton (Figure 2). With 1 mbar H_2S, the additional contribution is masked by the current density of proton reduction. However, at 9 mbar and 50 mbar H_2S, the second cathodic reaction is well defined, and its current increases with P_{H2S}. The cathodic current plateau associated with proton reduction is progressively hidden by the contribution due to H_2S reduction.

At pH 6 and without H_2S, the contribution of H^+ reduction to the global current rapidly vanishes and most of the cathodic current is associated with water reduction.
In the presence of dissolved H_2S, the cathodic contribution of the polarization curves can thus mostly be attributed to H_2S (Figure 3). Even though the plateau is not extremely well defined, the limiting current seems to be proportional to H_2S concentration. The impact of H_2S on the kinetic part could also be estimated from the results at 9 mbar and 50 mbar of H_2S, which present a linear region at low overpotential. From the values of the cathodic current at -0.6 V vs. Ag/AgCl, the order of the reaction with C_{H2S} could be estimated as:

$$\frac{\partial \log\left(J_{0,H_2S}\right)}{\partial \log\left(C_{H_2S}\right)} \approx 0.5 \qquad (11)$$

This reaction order is equivalent to that of the exchange current density of proton reduction in similar environments, as already mentioned by several authors [6,10,23]:

$$\frac{\partial \log\left(J_{0,H^+}\right)}{\partial \log\left(C_{H^+}\right)} \approx 0.5 \qquad (12)$$

The stationary cathodic polarization curves in the limiting current domain are plotted in Figure 4 for different rotation rates of the electrode at pH 6 and with 50 mbar H_2S. From these experiments, the values of the limiting current density measured at -1.05 V vs. Ag/AgCl are plotted versus the square root of the electrode rotation rate (Figure 5). In the same figure, the theoretical mass transport limiting current for H_2S calculated with the Levich relation (11) was also plotted for comparison.

$$J_{\lim,H_2S} = 0.62FC_{H_2S_{bulk}} D_{H_2S}^{2/3} \upsilon^{-1/6} \omega^{1/2} \qquad (13)$$

with $J_{\lim,H_2S}$ the diffusion limited current for H_2S reduction, $C_{H_2S_{bulk}}$ the H_2S concentration in the bulk of the solution (5 x 10^{-3} mol/L for P_{H2S} = 50 mbar), and D_{H_2S} the diffusion coefficient of H_2S (1.6 x 10^{-5} cm²/s [9]).

It appears quite clearly in Figure 5 that the experimental data stay below the theoretical line, and that the difference between measured and calculated values seems to increase with rotation speed. The current limitation is then not just caused by H_2S transport, but might also contain an additional contribution due to homogeneous H_2S dissociation (reaction 8).

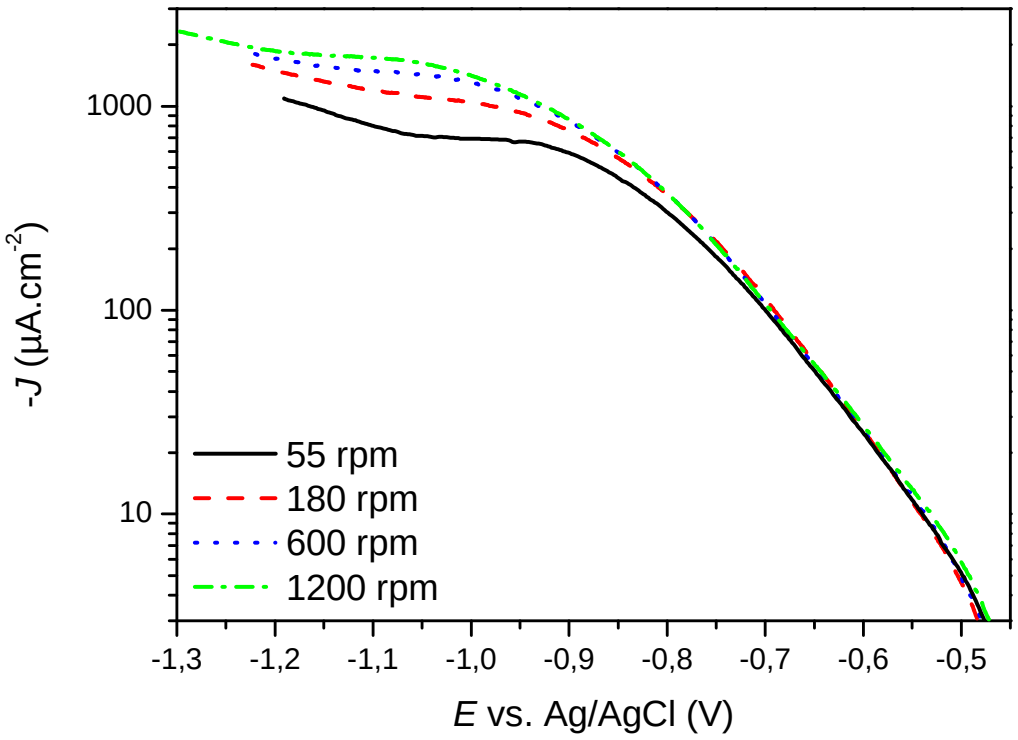

Figure 4: Experimental stationary cathodic polarization curves measured with a RDE at different rotation speed in de-aerated solution containing at pH 6 with 50 mbar H_2S

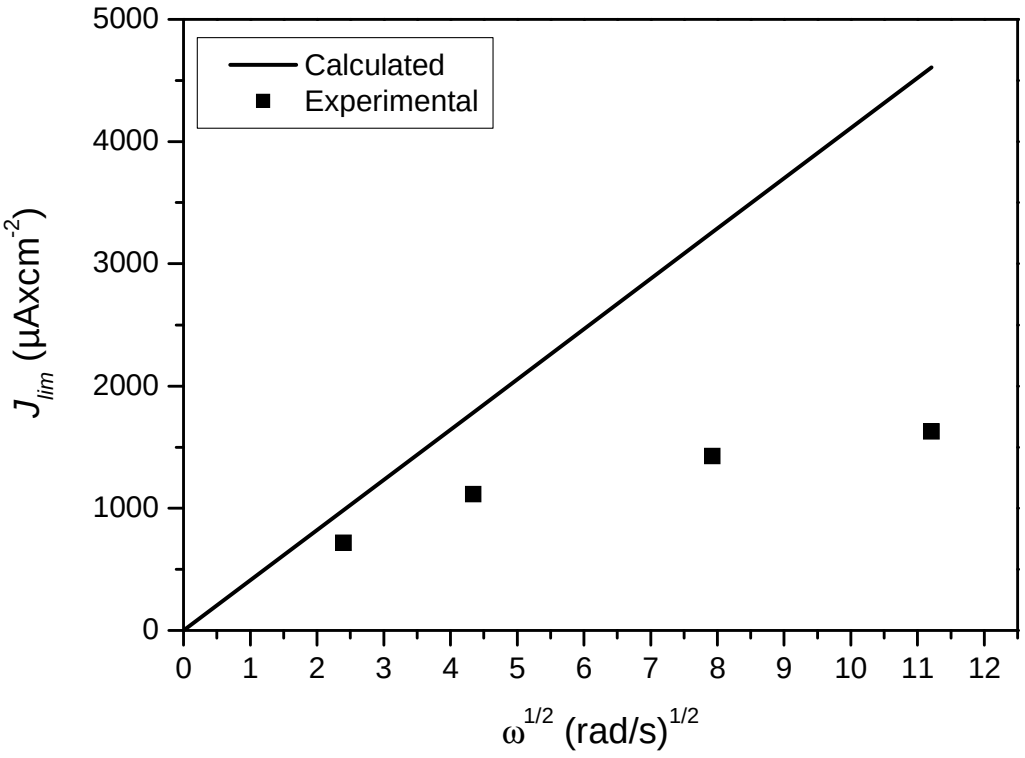

Figure 5: Evolution of the limiting cathodic current with the rotation speed of the electrode in de-aerated solution containing at pH 6 with 50 mbar H_2S

After the analysis of the plateau region, we examined the apparent kinetic part of the polarization curves related to the reduction reaction involving H_2S. In order to correct for mass transfer limitation, the Tafel correction was applied in the low overpotential region to calculate the kinetic current density as:

$$J_{k,H_2S} = \frac{J \times J_{\lim,H_2S}}{J_{\lim,H_2S} - J} \qquad (14)$$

where J_{k,H_2S} is the kinetic part of the cathodic current density and J is the global measured current density after ohmic drop compensation.

The results are plotted in Figure 6 for different rotation rates, for the experiments at pH 6 and with 50 mbar H_2S. An excellent agreement is found between the different sets of results, and an apparent Tafel slope equal to 145 ± 10 mV is derived. This high value suggests that for the results of Figure 4, the linear part of $\log(J)$ vs. E is not under pure activation control, but contains an additional contribution. At this stage, it is not possible to precisely define this contribution, but cathodic current due to water and residual H^+ reduction might have an influence, as well as some residual O_2 reduction in case of small O_2 pollution of the system. A rough estimate of the additional contribution to H_2S reduction could be made from the measurements in dilute H_2SO_4

at pH 6 in Figure 3. In the linear region used for the Tafel analysis, between -0.55 and -0.75 mV vs. Ag/AgCl, the residual reduction current due to H^+, H_2O and other species in the solution varies from 5 to 20 µA/cm². This results in an overestimate of the Tafel slope with Equation (12). Unfortunately, the reproducibility of the measurements in dilute acid solution at pH 6 was not sufficient to perform a correction of the measured current in Equation (12). Nevertheless, a Tafel value of 120 mV for H_2S is likely, similar to that of the proton reduction.

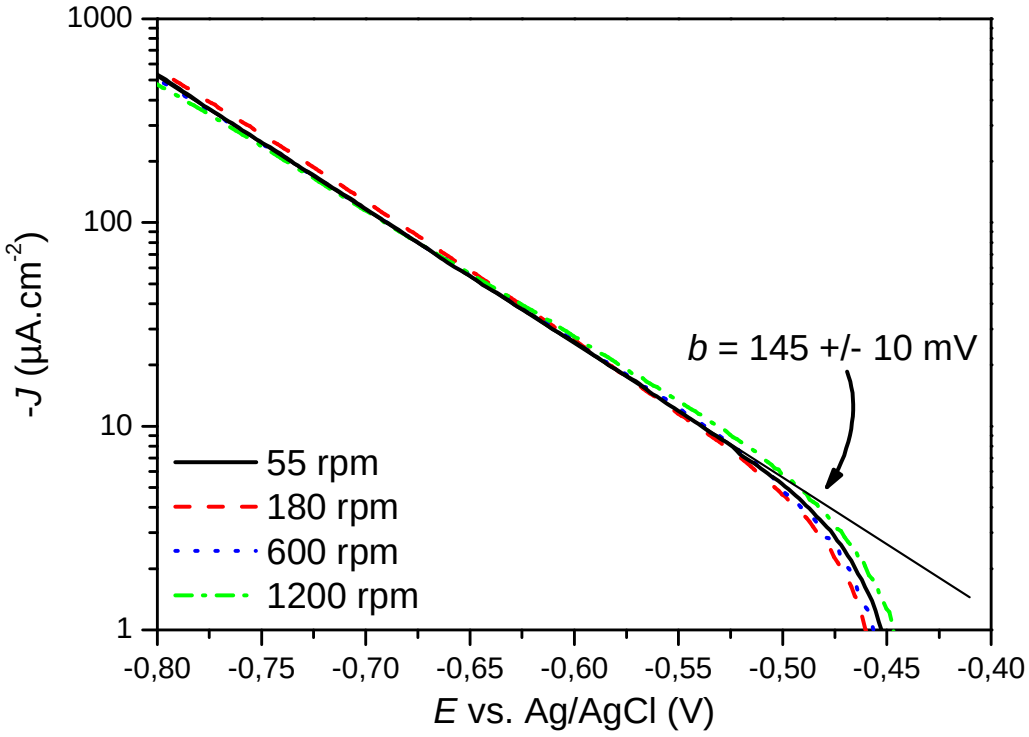

Figure 6: Tafel plots of the kinetic part of the cathodic current (J_k) in pH 6 solution saturated with 50 mbar H_2S

Modelling approach

In a previous paper, we have shown that cathodic reactions in acid water containing dissolved CO_2 could be described by a simple coupled chemical – electrochemical model, with proton reduction as unique cathodic reaction [10]. The results presented in this paper clearly show that the same reaction scheme is not sufficient to describe electrochemical reactions with dissolved H_2S. In particular, a direct reduction of H_2S or HS^- has to be considered.

Although it was not solved numerically, the main reactions and equations necessary to describe cathodic reactions at the surface of a rotating disc electrode in acid water containing H_2S are presented in this section. Numerical simulation with the different hypothesis for H_2S reduction will be presented in a future paper.

General assumptions

The system could be modelled as depicted in Figure 7. It consists of a non reactive rotating disc electrode immersed in a solution saturated with H_2S. The stationary state is supposed to be reached.

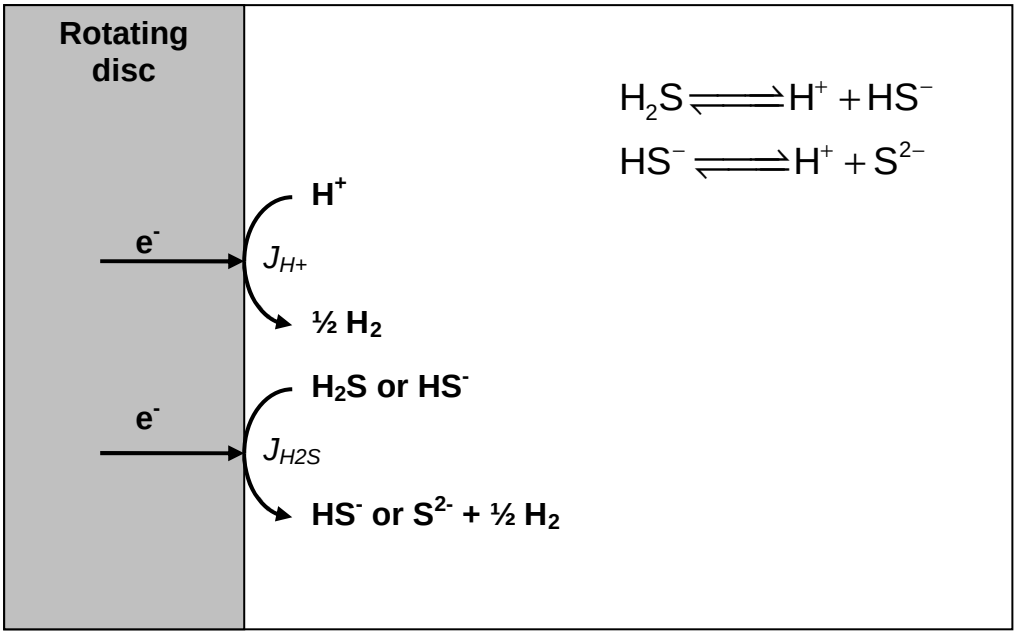

Figure 7: Scheme of the system describing cathodic reactions in acid water containing dissolved H_2S

According to Nordsveen et al. [9], the current density of proton reduction corresponding to reaction (2) is given by:

$$J_{H^+} = k_{H^+} C_{H^+(x=0)}^{0.5} 10^{\left(\frac{-E}{b_{c,H^+}}\right)} \qquad (15)$$

where k_{H^+} is the cathodic rate constant of H^+ reduction, $C_{H^+(x=0)}$ is the proton concentration at the electrode surface, E is the electrode potential, and b_{c,H^+} is the cathodic Tafel slope for H^+ reduction.

In addition to the cathodic reduction of H^+ an additional electrochemical reaction with H_2S has to be considered.
This reaction could be a direct reduction of H_2S (reaction 6), as proposed by Bolmer [14]. However, HS^- is also likely to be reduced:

$$HS^- + e^- \rightarrow S^{2-} + \frac{1}{2}H_2 \quad (16)$$

Indeed, HS^- is produced from H_2S dissociation by reaction 8, and the local concentration of HS^- increases with the pH. At the steel surface, as the pH increases due to H^+ reduction, HS^- concentration could then rapidly become significant compared to H_2S concentration.

The current density for either of these reactions could be expressed by a similar expression as proton reduction:

$$J_{H_2S} = k_{H_2S} C_{H_2S(x=0)}^{\alpha_{H_2S}} 10^{\left(\frac{-E}{b_{c,H_2S}}\right)} \quad (17)$$

where k_{H_2S} is the cathodic rate constant of H_2S or HS^- reduction, $C_{H_2S(x=0)}$ is the H_2S or HS^- concentration at the electrode surface, α_{H_2S} is the reaction order and is equal to 0.5 according to our experimental results, E is the electrode potential, and b_{c,H_2S} is the cathodic Tafel slope.

Homogeneous chemical reactions of H_2S dissociation (reaction 8 and 9) must also be considered in the model. As in the case of CO_2 [10], it is not postulated that these reactions always stand at thermodynamic equilibrium. It could thus be necessary to consider the chemical kinetics expressions:

$$R_1 = k_1 C_{H_2S} - k_{-1} C_{HS^-} C_{H^+} \quad (18)$$

$$R_2 = k_2 C_{HS^-} - k_{-2} C_{S^{2-}} C_{H^+} \quad (19)$$

where R_1, k_1 and k_{-1} are respectively the rates of the reaction and the forward and backward kinetic constants for H_2S dissociation (Reaction 8), and where R_2, k_2 and k_{-2} have the same meaning for HS^- dissociation (Reaction 9). Although the kinetic rate constants for these reactions are not well documented in the literature, it is often postulated that the dissociation of H_2S is much faster than that for CO_2 [9].

Governing equations

The governing equations of the system are the mass balance equations expressed for each species *i* of the model. These equations can be written according to:

$$-D_i \frac{\partial^2 C_i}{\partial x^2} + V_x \frac{\partial C_i}{\partial x} = R_i \quad (20)$$

with D_i the diffusion coefficient of species i, C_i its concentration, V_x the convective transport rate in the direction normal to the electrode surface, and R_i the homogeneous production rate, determined from (18) and (19) with the following relations:

$$R_{H^+} = R_1 + R_2 \tag{21}$$

$$R_{H_2S} = -R_1 \tag{22}$$

$$R_{HS^-} = R_1 - R_2 \tag{23}$$

$$R_{S^{2-}} = -R_2 \tag{24}$$

According to Levich [24], the convection term for a rotating disc electrode can be expressed as:

$$V_x = -0.510 \upsilon^{-1/2} \omega^{3/2} x^2 \tag{25}$$

where υ is the kinematic viscosity of the solution, ω is the angular rotation speed of the electrode, and x is the normal distance to the electrode surface.

The complete system is described by a set of four coupled non linear differential equations (20) for H_2S, HS^-, S^{2-}, H^+, with chemical production or consumption terms given above.

Boundary conditions

Solving the system requires to define boundary conditions.

Far from the electrode, it is reasonable to consider that thermodynamic equilibrium is reached. Thus, for a given pH and a given partial pressure of H_2S (P_{H2S}), the bulk concentration of different species can easily be calculated as:

$$C_{H_2S} = H_{H_2S} P_{H_2S} \tag{26}$$

$$C_{HS^-} = K_1 \frac{C_{H_2S}}{C_{H^+}} \tag{27}$$

$$C_{S^{2-}} = K_2 \frac{C_{HS^-}}{C_{H^+}} \tag{28}$$

where H_{H_2S} is the Henry's constant for H_2S, and K_1 and K_2 are respectively the equilibrium constants of reaction (8) and reaction (9).

At the electrode surface, the flux of non-electroactive species is necessarily equal to zero, which is mathematically equivalent to:

$$\frac{\partial C_{OH^-}}{\partial x} = 0 \qquad (29)$$

On the other hand, the flux of H^+ is given by (15), while the flux of H_2S or HS^- is given by (17).
If one considers H_2S reduction, HS^- is produced by H_2S reduction (reaction 6). Then HS^- flux at the steel surface is produced, with the same value but an opposite sign as the H_2S reduction flux. In that case, S^{2-} is non electroactive, and reaction (29) also applies.
On the other hand, if one considers HS^- reduction, H_2S becomes non electroactive, and two electrochemical fluxes are found at the steel surface for HS^- and S^{2-}.
These different hypothesis are planned to be examined numerically in a future paper.

Conclusions

The hydrogen evolution reaction in an oxygen free solution with dissolved H_2S is radically different than with dissolved CO_2, even though both dissolved gases are weak acids with comparable solubility and pKa. With dissolved CO_2, proton reduction is the main cathodic reaction. Dissolved CO_2 only contributes to increase the current density in the mass transfer control potential range by a chemical buffer effect. In this potential domain, the transport of the weak acid is added to the transport of proton, and additional interfacial acidity is provided by the weak acid dissociation.
On the contrary, the results presented in this paper demonstrate that the buffer effect is not sufficient to explain cathodic polarization curves measured in solutions with dissolved H_2S. An additional cathodic reaction was clearly observed. Although our results did not allow characterizing completely this electrochemical reaction, some apparent features could be determined. This reaction presents strong links with H_2S concentration. The reaction order with C_{H2S} seems to be close to 0.5. A cathodic current plateau was also observed at high cathodic overpotential, but the relationship with H_2S diffusion was not straightforward. At low cathodic overpotential, a Tafel region was observed, with an apparent slope value of 145 ± 10 mV, suggesting also that the system was not strictly under activation control.

A model was proposed to describe reduction reactions in acid water containing dissolved H_2S. This model takes into account both the homogeneous chemical reactions of H_2S and HS^- dissociations, and the direct reduction of H_2S and H^+.

Acknowledgements

The authors kindly acknowledge Alexandre Bonneau for his active participation in the experimental part of this work. Elias Remita from Technip, is also thanked for fruitful discussion and for his participation at the beginning of the project.
The quality of this manuscript was greatly improved by helpful comments from S. Nesic, Y. Zheng, and J-L. Crolet.

References

1. C.Dewaard, D.E.Milliams, Carbonic-Acid Corrosion of Steel, Corrosion 31 (1975) 177-181
2. L.G.S.Gray, B.G.Anderson, M.J.Danysh, and P.R.Tremaine, Mechanisms of carbon steel corrosion in brines containing dissolved carbon dioxide at pH 4, *Corrosion/89*, paper n°464 (1989)
3. K.L.J.Lee and S.Nesic, The effect of trace amount of H_2S on CO_2 corrosion investigated by using EIS technique, *Corrosion 2005*, paper n°630 (2005)
4. B.R.Linter, G.T.Burstein, Reactions of pipeline steels in carbon dioxide solutions, Corrosion Science 41 (1999) 117-139
5. S.Nesic, B.F.M.Pots, J.Postlethwaite, N.Thevenot, Superimposition of diffusion and chemical reaction controlled limiting currents - Application to CO_2 corrosion, Journal of Corrosion Science and Engineering 1 (1995) paper n°3
6. S.Nesic, J.Postlethwaite, S.Olsen, An electrochemical model for prediction of corrosion of mild steel in aqueous carbon dioxide solutions, Corrosion 52 (1996) 280-294
7. S.Nesic, J.Postlethwaite, M.Vrhovac, CO_2 corrosion of carbon steel - from mechanistic to empirical modelling, Corrosion Reviews 15 (1997) 211-240
8. S.Nesic, H.Li, J.Huang, and D.Sormaz, An open source mechanistic model for CO_2 / H_2S corrosion of carbon steel, *Corrosion 2009*, paper n°572 (2009)
9. M.Nordsveen, S.Nesic, R.Nyborg, A.Stangeland, A mechanistic model for carbon dioxide corrosion of mild steel in the presence of protective iron carbonate films - Part 1: Theory and verification, Corrosion 59 (2003) 443-456
10. E.Remita, B.Tribollet, E.Sutter, V.Vivier, F.Ropital, J.Kittel, Hydrogen evolution in aqueous solutions containing dissolved CO_2: Quantitative contribution of the buffering effect, Corrosion Science 50 (2008) 1433-1440
11. G.Schmitt, B.Rothman, Studies of the corrosion mechanism of unalloyed steels in oxygen-free carbon dioxide solutions. Part I. Kinetics of the liberation of hydrogen, Werkstoffe und Korrosion 28 (1977) 816-822
12. G.A.Zhang, Y.F.Cheng, On the fundamentals of electrochemical corrosion of X65 steel in CO_2-containing formation water in the presence of acetic acid in petroleum production, Corrosion Science 51 (2009) 87-94
13. T.Tran, Mechanistic study of cathodic reaction in sweet corrosion, *Corrosion 2012*, Poster presentation (2012)
14. P.W.Bolmer, Polarization of iron in H_2S-NaHS buffers, Corrosion 21 (1965) 69-75
15. D.R.Morris, L.P.Samplaleanu, D.N.Veysey, The corrosion of steel by aqueous solutions of hydrogen sulfide, Journal of the Electrochemical Society 127 (1980) 1223-1235
16. R.Galvan-Martinez, J.Mendoza-Flores, R.Duran-Romero, J.Genesca, Effect of turbulent flow on the anodic and cathodic kinetics of API X52 steel corrosion in H_2S containing solutions. A rotating cylinder electrode study, Materials and Corrosion 58 (2007) 514-521
17. D.W.Shoesmith, P.Taylor, M.G.Bailey, D.G.Owen, The Formation of Ferrous Monosulfide Polymorphs During the Corrosion of Iron by Aqueous Hydrogen-Sulfide at 21-Degrees-C, Journal of the Electrochemical Society 127 (1980) 1007-1015
18. W.Sun and S.Nesic, A mechanistic model of H_2S corrosion of mild steel, *Corrosion 2007*, paper n°655 (2007)

19. C.Azevedo, P.S.A.Bezerra, F.Esteves, C.J.B.M.Joia, O.R.Mattos, Hydrogen permeation studied by electrochemical techniques, Electrochimica Acta 44 (1999) 4431-4442
20. B.J.Berkowitz, H.H.Horowitz, The role of H_2S in the corrosion and hydrogen embrittlement of steel, Journal of the Electrochemical Society 129 (1982) 468-474
21. R.N.Iyer, I.Takeuchi, M.Zamanzadeh, H.W.Pickering, Hydrogen sulfide effect on hydrogen entry into iron - A mechanistic study, Corrosion 46 (1990) 460-468
22. B.Le Boucher, Etude du dégagement cathodique de l'hydrogène sur le fer en présence d'hydrogène sulfuré, Revue de l'Institut Francais du Petrole 23 (1963) 1-66
23. J.O.Bockris, D.Drazic, A.R.Despic, The electrode kinetics of the deposition and dissolution of iron, Electrochimica Acta 4 (1961) 325-361
24. V.G.Levich, "Physicochemical Hydrodynamics", Prentice Hall, Englewood Cliffs,New Jersey (1962)
25. Y.Zheng, Electrochemical mechanisms of H_2S corrosion of carbon steel, *Corrosion 2012*, Poster presentation (2012)